Validation of a field deployable reactor for *in situ* formation of NOM-engineered nanoparticle corona†

Narjes Tayyebi Sabet Khomami, [a] Allan Philippe, [*a] Abd Alaziz Abu Quba,[a] Oliver J. Lechtenfeld,[bc] Jean Michel Guigner,[d] Stefan Heissler[e] and Gabriele E. Schaumann[a]

Despite the numerous studies about the sorption of dissolved organic matter (DOM) onto nanoparticles, the extrapolation of laboratory results to environmental conditions is currently impossible. Indeed, the complex dynamics of DOM under variable environmental conditions are not completely reproducible under control conditions. In this study, we propose a different approach by exploring a method for exposing nanoparticles to realistic environmental conditions in natural river water by using dialysis membranes as passive reactors. Inside this reactor, the complexity and the temporal variability of a large number of environmental parameters (DOM structure and composition, temperature, inorganic ions, pH, *etc.*) are reproduced, while colloidal and particulate interferences remain separated. To verify this assumption, we determined the concentration of the water components and nanoparticles (n-TiO$_2$, 20 50 nm) inside and outside the reactor before and after exposure to river water. In river water, more than 90% of the n-TiO$_2$ nanoparticles remained inside the reactor while DOM retained its molecular composition/characteristics after passing through the membrane (DOC, fluorescence EEM, and FT-ICR MS). For most elements and anions, the concentrations inside and outside the reactor did not differ, indicating a good permeability for inorganic constituents (IC, ICP-OES); however, the concentrations of Al, Fe, Mn, and nitrate were lower. Membrane fouling, in terms of pore size distribution, was investigated using NMR relaxometry and AFM in fluid mode; no significant reduction in pore size was observed under the applied conditions during seven days of exposure. Finally, ATR-FTIR and CHNS analysis of n-TiO$_2$ before and after exposure to the river water revealed that sorption of DOM occurred under field conditions. Therefore, we could demonstrate the validity and the potential of this method.

Environmental significance

The release of nanoparticles to surface waters is inevitable. Studies about the interactions of nanoparticles with organic matter in the river water were usually conducted in the lab under controlled conditions. Here, we propose a realistic exposure of nanoparticles to river water by using dialysis bags as passive reactors to study the sorption of DOM of river water onto n TiO$_2$. The concept is simple and easily applicable to a broad range of nanoparticles and surface waters and, hence, can provide a better understanding of how NOM corona develops on nanoparticles under field conditions. This will help in predicting their environmental fate and impact.

[a] iES Landau, Institute for Environmental Sciences, Koblenz Landau University, Fortstrasse 7, 76829 Landau, Germany. E mail: philippe@uni landau.de
[b] UFZ Helmholtz Centre for Environmental Research, Department Analytical Chemistry, Research Group BioGeoOmics, 04318 Leipzig, Germany
[c] ProVIS Centre for Chemical Microscopy, UFZ Helmholtz Centre for Environmental Research, 04318 Leipzig, Germany
[d] IMPMC, Sorbonne University, CNRS UMR 7590, MNHN, Paris, France
[e] Institute of Functional Interfaces IFG, Karlsruhe Institute of Technology KIT, Hermann von Helmholtz Platz 1, D 76344 Eggenstein Leopoldshafen, Germany

Introduction

For the last 15 years, engineered nanomaterials (ENMs) have attracted growing academic and industrial interest with a wide range of applications in cosmetics, building materials, medicine, and energy storage.[1] Among these materials, titanium dioxide nanoparticles (n-TiO$_2$) represent the second most important part of ENM production worldwide (550–5500 t per year) which is expected to increase in the near future.[2–4] This high production as well as diverse applications leads to inevitable emission of n-TiO$_2$ into the

environment. These nanoparticles can enter aquatic systems either directly or indirectly *via* wastewater treatment plants or landfills.[5–7]

The fate and biological activity of n-TiO$_2$ in aquatic systems depend not only on nanoparticle properties, but also on the characteristics of the receiving water environment including dissolved organic matter (DOM), multivalent cations and natural colloids.[8] DOM, mainly containing humic substances, polysaccharides, and proteins, represents one of the most dynamic fractions of organic matter in aquatic systems. Depending on the biochemical conditions and concentration in waters, they typically range from 0.1 to 10 mg L^{-1}.[9] Once n-TiO$_2$ nanoparticles are released into natural systems, interactions of NOM with these nanoparticles will affect their fate, transport, and risk assessments.[10] There are a multitude of studies to understand NOM sorption on titanium dioxide nanoparticles;[10–17] nonetheless, most of them have been conducted in the laboratory under highly simplified controlled conditions which do not consider, for instance, DOM dynamic structure dependency on water parameters affecting the sorption mechanism. Therefore, the results are difficult or even impossible to extrapolate to natural conditions. Hence, there is still a lack of methods allowing a realistic exposure of nanoparticles to temporal environmental conditions including NOM composition, temperature, background electrolyte concentration, and pH for testing hypotheses developed from lab experiments.

Passive sampling is an environmental monitoring technique based on free flow of analyte molecules from the sampled medium to a collecting medium as a result of a difference in chemical potentials.[18–20] The device used for passive sampling is usually a dialysis membrane.[20] Dialysis is a simple process in which small solutes diffuse from a high concentration solution to a low concentration solution across a semipermeable membrane. There are several studies using dialysis membranes in passive sampling. Vroblesky *et al.* used regenerated cellulose dialysis samplers to measure volatile organic compounds in different wells.[21] Vencalek *et al.* applied cellulose ester dialysis bags to separate Cu nanoparticles from the dissolved Cu species in freshwater mesocosms.[22] Benes *et al.* determined the state of trace elements in natural waters using a cellulose membrane.[23]

In this study, we present the first steps of the evaluation of a realistic river water exposure method for n-TiO$_2$ inspired by the concept of passive sampling. n-TiO$_2$ nanoparticles were selected to test the method since they do not dissolve in water and the sorption of DOM components on these nanoparticles is well studied.[24,25] The proposed method relies on membrane dialysis, *i.e.* the dialysis bag is considered as a passive reactor retaining n-TiO$_2$ nanoparticles inside while DOM can diffuse inside. Furthermore, natural colloids cannot enter which simplifies the extraction of the nanoparticles after exposure. In order to apply this method to environmental waters, the membrane needs to meet several requirements:

- Retain nanoparticles and permeable to non-colloidal water components (suitable molecular weight cut-off of the membrane)
- Robustness towards environmental variation (pH, temperature, water flow, and aquatic organisms)
- The permeability of the membrane should remain constant during the exposure. Fouling is the principal mechanism affecting the permeability under environmental conditions.[26,27]

In order to assess these issues, we exposed the dialysis bags (for improved readability, we will refer to "dialysis bag" for denoting the passive reactor) to river water and determined the concentration of the main organic and inorganic components inside and outside. Furthermore, we investigated the pore structure before and after exposure using NMR relaxometry and AFM in fluid mode.

Finally, we carried out a field exposure of n-TiO$_2$ to a river and evaluated the sorption of DOM of the river water onto n-TiO$_2$ by characterizing the nanoparticles before and after river exposure using ATR-FTIR and CHNS analyses. The results present the proof-of-concept of using dialysis bags and the validity of implementing this method to study the interactions of NOM and engineered nanoparticles under real environmental conditions.

Materials and methods

Materials

Biotech cellulose ester (CE) membranes with three different molecular weight cut offs (20, 100, and 300 kDa) were purchased from Repligen (Formerly Spectrum). The specifications provided by the supplier can be found in Table 1. Before usage, the membranes were soaked first in 10% (v/v) ethanol–water for 10 minutes, rinsed with distilled water (DW) and soaked in DW for removing glycerin and achieving maximum membrane permeability.[28] The membranes were stored in DW until further usage. Pre-experiments with dialysis bags using clip type closure resulted in the loss of 50% of the deployed dialysis bags, damaged under the movement induced by the river flow (30–40 cm s^{-1}, OTT MF pro, Germany). Therefore, cylindrical dialysis bags with screw-on caps showing 100% resistance over one week were selected for this study (Fig. S1†). Aeroxide® n-TiO$_2$ P25 powder was purchased from Degussa, Germany.

HR-TEM (n-TiO$_2$)

For nanoparticle characterization, 5 μL of 1 g L^{-1} n-TiO$_2$ suspension was placed on a TEM grid and dried under ambient conditions. Transmission electron microscopy (TEM) measurements were performed using a JEOL 2100F (JEOL Ltd., Tokyo, Japan) field emission gun instrument operating at 200 kV equipped with a polar piece of ultra-high resolution. Images were recorded on an UltraScan 4000 Gatan (Gatan Inc., Pleasanton, CA, United States) camera with a 4k × 4k pixel CCD.

Table 1 Specifications of the dialysis bag

Specifications	Membrane type	Physical appearance	Packaging	pH limit	Temperature limit	Total length	Membrane diameter
	Float A Lyzer® cellulose ester (CE)	Opaque, rigid	Dry with glycerine	2 9	4 37 °C	10 cm	10 mm

Sampling and characterization of the river water

The experiments were conducted with water collected from the River Queich (latitude: 49.205510, longitude: 8.088081) in Landau in der Pfalz, Germany in May–September 2018 (in case of a complementary experiment, the date is mentioned). For the sake of simplicity, we will refer to "river water" for denoting the water sampled at this place. The characteristics of the river water were fairly stable over this period of time (Table S1†).

Samples were collected in a polypropylene canister at 1 m from the river bank. The pH was measured on site (SG2-FK SevenGo, Mettler Toledo, Schwerzenbach, Switzerland). The samples were transported immediately to the nearby laboratory, and were stored in the dark at 4 °C. A multi-parameter analyser (Consort C863, Turnhout, Belgium) was used to measure electrical conductivity. Dissolved organic carbon (DOC) concentration was determined after filtration with 0.45 μm PTFE filters (Altmann, Germany) using a TOC analyzer (multi N/C 2100, Analytik Jena AG, Jena, Germany). The concentrations of Al, Ba, Ca, Cu, Fe, K, Mg, Mn, Na, Sr, and Zn the river water samples were measured using inductively coupled plasma optical emission spectroscopy (ICP-OES, 720, Agilent Technologies, Santa Clara, USA). The digestion procedure for determination was done similar to the literature with some modifications.[5] 10 mL of the river water was dried at 95 °C and cooled down at room temperature before adding 2.5 mL of hydrogen peroxide (30%, Rotipuran®, Carl Roth, Germany). After 10 min of standing at room temperature, 5 mL of sulfuric acid (95%, Rotipuran®, Carl Roth, Germany) was added dropwise before being progressively heated until ebullition (225 °C). After one hour at 225 °C, the samples were cooled down at room temperature and diluted into a 100 mL volumetric flask prior to ICP-OES analysis. All the samples were measured in triplicate. Ion chromatography (Professionel IC 881 Metrohm) was used to analyze anions. Dissolved oxygen was measured using a PyroScience optical oxygen sensor. The chemical and physical information of the river is summarized in Tables S1–S3.†

Permeability of dialysis bags toward n-TiO$_2$

To check the permeability of the dialysis bags for the nanoparticles used in this study, a 300 mg L^{-1} suspension of n-TiO$_2$ was prepared and sonicated (ultrasound bath) for 10 minutes. The dialysis bags were filled with 5 ml of n-TiO$_2$ suspension, and placed in a 50 ml polypropylene centrifuge tube filled with 35 ml river water. The tubes were shaken at 200 rpm using a horizontal shaker for a specified time. Samples were collected from outside of the dialysis bags, prior to Ti-content determination using ICP-OES. The samples were digested following Philippe *et al.*[5] The ICP-OES measurements were carried out for Ti at an emission wavelength of 334.941 nm. All the samples were measured in triplicate.

Determination of the equilibrium time

The dialysis bags were filled with 5 ml distilled water, and placed into a 50 ml polypropylene centrifuge tube filled with 35 ml river water. The tubes were shaken at 200 rpm using a horizontal shaker at room temperature (21 °C). After the specified time, samples were collected from inside and outside of the dialysis bags, filtered using 0.45 μm PTFE filters (Altmann, Germany), and analyzed for TOC.

NMR relaxometry

The transverse relaxation time (T_2) in ^{1}H NMR relaxometry measures the decay of magnetization of proton spins after excitation from their dephasing in time-dependent fluctuation of the magnetic field caused by adjacent nuclei (T_2).[29] Thus, the T_2 distribution can be related to the pore size distribution with the lower T_2 corresponding to water present in small pores while the larger T_2 corresponds to large pores as well as "free" bulk water. Cellulose compounds (dialysis bag) depict a recognizable bimodal T_2 distribution,[30] which was also observed for the cellulose ester membrane of the dialysis bag and represents the hierarchical porous structure of the membrane. For measuring the spin–spin relaxation time (T_2) of the dialysis bags in different media (distilled water and river water with and without n-TiO$_2$), the dialysis bags were completely emptied and measured immediately to avoid drying of the membrane. All the samples were measured in triplicate. A Bruker Minispec MQ, Version 2.2 (Bruker, Karlsruhe, Germany), was used at a magnetic field strength of 0.176 T (proton Larmor frequency of 7.5 MHz), applying 64 scans, with a recycle delay of 10 s. The gain was adjusted for each sample individually such that 70–80% signal intensity was achieved. Calculations were done and figures were processed using Matlab R2014 a and Origin 7.5, respectively.[31]

AFM

The dialysis bags were cut to approximately 2 × 1 cm^2 pieces. They were fixed on a steel-disc using instant glue, and stored in distilled water, or river water until measurement. Atomic force microscopy (AFM, Dimension Icon, Bruker Corporation, USA) analyses were conducted using tapping mode in water media, with New Sharp Nitride Lever tips (SNL, Bruker, USA)

with a radius of 2 nm (nominal value). Sample mounting for AFM fluid experiments along with the probe calibration procedures was performed as recommended in the Bruker protocols.[32,33] To measure the pore size of the dialysis bag, images were captured from six random locations and further processed for pore size estimation (ImageJ). The pore area was determined automatically after black/white picture conversion and contrast adjustment. The obtained areas were used to determine the hydrodynamic diameter for each pore (also known as pore thickness or opening diameter) defined as the diameter of the largest circle inscribed in a pore following eqn (1):

$$D_h = 4\frac{A}{P} \quad\quad (1)$$

where A (area) is the total number of pixels enclosed by the pore boundary, and P (perimeter) is the number of pixels on the boundary. The results of the six regions of interest were combined to have a set of representative data. Analysis of the images and corresponding calculations were carried out using the programs ImageJ v1.52a. and Origin 7.5.

Field exposure experiment

To avoid the damage of dialysis bags by the stream flow of the river or aquatic animals, each dialysis bag was enclosed in a perforated polyethylene plastic canister (approximate perforation diameter: 0.3 mm). The dialysis bags were filled with 5 ml distilled water (control), or a freshly prepared and sonicated (10 minutes in an ultrasound bath) n-TiO$_2$ 300 mg L^{-1} suspension (three replicates), and placed in the canister (Fig. S2†). The canisters were fixed to an anchor and immersed in the river about 1 m from the river bank. After a week, the content of the dialysis bags was collected in a 15 mL polypropylene centrifuge tube and immediately transferred to the laboratory for further analyses. It is worth mentioning that the realistic concentration of n-TiO$_2$ in surface waters is low (e.g. 0.55–16 μg L^{-1}).[34] However, the majority of current analytical techniques used for sorption studies are not capable of working with concentrations in the μg L^{-1} range; therefore, the applied n-TiO$_2$ concentration (300 mg L^{-1}) was way too high compared with the realistic ones. Nonetheless, in the field experiment, there is a large excess of available DOM for nanoparticles; hence, the high concentration of n-TiO$_2$ (300 mg L^{-1}) inside the bags does not change the ratio of sorbate/sorbent significantly.

Fluorescence spectroscopy

The collected river water samples were centrifuged (Universal 320, Hettisch, Bäch, Switzerland) at 4500 rpm (3283 g) for 30 min. Since the n-TiO$_2$ nanoparticles were visibly agglomerated, this speed was sufficient to collect them at the bottom and the supernatant was transparent under these conditions. The supernatant was taken for further measurements. The fluorescence excitation/emission matrix (EEM) of the samples was recorded on a PerkinElmer LS 55 fluorescence spectrometer in the emission (Em) range of 200–700 nm by varying the excitation (Ex) wavelength from 250 to 450 nm in 20 nm increments with a scan rate of 1200 nm min^{-1}. Excitation and emission slits were both 10 nm. Since a linear calibration curve (fluorescence intensity versus fluorophore concentrations, $R^2 = 0.9991$) was obtained after serial dilutions of the river water, we considered the filter effects as negligible for this river sample. No corrections for scattering effects were applied to the data as there was no observable overlapping of the fluorescence and scattering peaks. The EEM spectra were plotted using Origin 7.5.

CHNS

For each measurement of the river water, 250 ml of the river water was filtered with 0.45 μm PTFE filters (Altmann, Germany), and freeze-dried (Christ, Osterode, Germany) for two continuous days at 40 °C and 0.12 mbar and two more days at 60 °C and 0.011 mbar. The TiO$_2$ nanoparticles exposed to the river water were centrifuged at 4500 rpm (3283g) for 30 min. The supernatant was withdrawn carefully to the last drop and the centrifugate was freeze dried as described above. For CHNS elemental analysis, 4–15 mg of samples were weighed into tin boats (LabNeed GmbH, Nidderau, Germany) together with around 20 mg of WO$_3$ powder (LabNeed GmbH, Nidderau, Germany), and measured using a CHNS varioMicroCUBE (Elementar, Langenselbold, Germany). Sulfanilamide (Elementar GmbH, Langenselbold, Germany) was used as a reference sample. Computation of the Euclidian distances was carried out using the program R Studio (Version 1.0.143).

ATR-FTIR

The nanoparticle pellet collected after centrifugation and also the river water sample collected on the last day of the field experiment were freeze-dried as with CHNS analysis. For ATR-FTIR measurements, a Bruker Tensor 27 IR spectrometer (Bruker Optics, Ettlingen, Germany) with a Bruker Platinum ATR accessory, single reflectance diamond crystal, 45° angle of incidence, was used. Some milligrams of the samples were applied directly on the ATR-crystal. Spectra were measured against an air background. Each spectrum comprised 32 coadded scans with a spectral resolution of 4 cm^{-1} in the 3600–370 cm^{-1} range. The absorption spectra were obtained using Origin 7.5 software.

FT-ICR-MS sample preparation and measurement

River water samples (5 mL) were extracted via solid-phase extraction using an automated sample preparation system (FreeStyle, LC Tech) on 50 mg styrene–divinyl–polymer type sorbents (Bond Elut PPL, Agilent Technologies) to desalt the sample for subsequent DI-ESI-MS according to Raeke et al.[35] The SPE-DOM was eluted with 1 mL methanol (Biosolv), diluted to 20 ppm and mixed at 1 : 1 (v/v) with ultrapure water immediately prior to FT-ICR MS analysis. Carbon based extraction efficiency was approx. 50% (for river water). SRFA

measured in triplicate was used to check instrument variability and solvent and extraction blanks were prepared.

An FT-ICR mass spectrometer equipped with a dynamically harmonized analyzer cell (solariX XR, Bruker Daltonics Inc., Billerica, MA) and a 12 T refrigerated actively shielded superconducting magnet (Bruker Biospin, Wissembourg, France) was used in ESI negative mode (capillary voltage: 4.3 kV). Extracts were analyzed in random order with an autosampler (infusion rate: 10 μL min^{-1}). For each spectrum, 256 scans were co-added in the mass range 150–3000 m/z with 25 ms ion accumulation time and 4 MW time domain (resolution@400 m/z $ca.$ 500 000). Mass spectra were internally linearly calibrated with a list of peaks (250–600 m/z, $n > 143$) commonly present in terrestrial DOM and the mass accuracy after calibration was better than 0.13 ppm. Peaks were considered if the signal/noise (S/N) ratio was greater than four.

FT-ICR-MS data evaluation

Molecular formulas were assigned to peaks in the range 150–750 m/z allowing for elemental compositions C_{1-60} $^{13}C_{0-1}$ H_{1-122} O_{1-40} N_{0-2} S_{0-1} $^{34}S_{0-1}$ with an error range of ±0.5 ppm according to Lechtenfeld et $al.$[36] Briefly, the following rules were applied: $0.3 \leq H/C \leq 2.5$, $0 \leq O/C \leq 1.0$, $0 \leq N/C \leq 1.5$, $0 \leq DBE \leq 20$ (double bound equivalent, DBE = 1 + 1/2 (2C H + N), Koch et $al.$[37]), $8 \leq DBE\text{-}O \leq 8$ (Herzsprung et $al.$[38,39]), and element probability rules proposed by Kind and Fiehn.[40] Isotope formulas were used for quality control but removed from the final data set as they represent duplicate chemical information. All molecular formulas present in the medium blank or instrument blank samples were excluded from the peak lists. 4668–5022 formulas were assigned with no multiple assignments to 16 568–17 423 peaks above the noise level. Molecular formulas and compounds are used synonymously throughout the text, although no molecular structures are known.

Relative peak intensities were calculated based on the summed intensities of all assigned monoisotopic peaks in each sample. Van Krevelen diagrams for river water samples inside and outside the dialysis bags were used to depict differences in relative intensities (ΔRI) for each individual molecular formula according to eqn (2).[41]

$$\Delta RI = \frac{\text{sample}}{(\text{sample} + \text{reference})} \qquad (2)$$

where sample refers to the water inside the bag (with n-TiO$_2$) and reference is the water outside the bag (river water). To test the effect of instrumental variability on the ΔRI values, six SRFA samples (Suwannee River fulvic acid) were measured on the same day. Relative standard deviations (RSDs) were calculated from the normalized intensities for each molecular formula. The 95 percentile of the RSD values was used as the threshold and any change in normalized peak intensity among different samples above this percent value is considered as statistically significant (Fig. S3†). ΔRI values corresponding to the RSD threshold were calculated (ΔRI < 0.43; ΔRI > 0.57). In the following, ΔRI values above 0.57 were considered to indicate that the respective compound is enriched in the sample, and ΔRI values below 0.43 indicate that the respective compound is enriched in the reference.

Results and discussion

Permeability of the membrane

The selection of an appropriate dialysis membrane is essential for exposing nanoparticles to DOM under field conditions. In particular, the molecular weight cut-off (MWCO) should be high enough for the dissolved components of natural water to diffuse freely through the membrane, to simulate the river composition to a good extent inside the dialysis bag. On the other hand, the membrane should not be permeable towards nanoparticles, in this study represented by n-TiO$_2$.

Fig. 1 shows the HR-TEM image of pristine n-TiO$_2$ with diameters in the range of 20–50 nm. Hence, the average pore size of the applied dialysis bag should be significantly lower than 20 nm to retain the nanoparticles. Symmetrically, natural colloids larger than the membrane pore size will not permeate through the membrane, thus simplifying the analytical procedure for the subsequent surface analysis of the DOM-coated nanoparticles.

Table 2 shows the retention rate of n-TiO$_2$ depending on the MWCO (20, 100, and 300 kDa) after two and seven days of exposure. The initial Ti-content of river water was below the detection limit of ICP-OES (Table S2†). The retention rates were all higher than 90%. High retention values are expected considering the smaller size of n-TiO$_2$ (20–50 nm) compared to the pore size of the membranes (5–20 nm). Furthermore, n-TiO$_2$ nanoparticles agglomerated in the river water due to the almost neutral pH (close to the isoelectric point of P25)[42] and the presence of different ions.[24] Therefore, the non-permeability of the membrane to nanoparticles can be improved when the nanoparticles agglomerate in the natural water. Hence, the colloidal stability in natural water has to be considered in the choice of the membrane cut-off in addition to the size of primary particles.
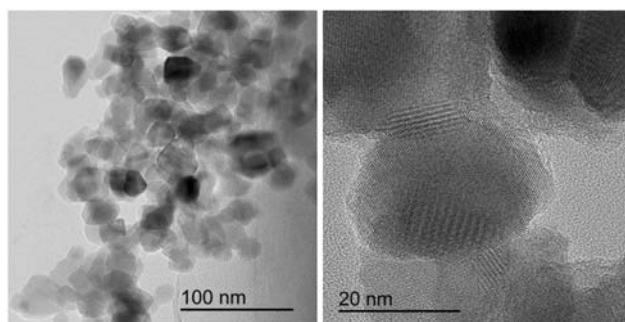

Fig. 1 HR TEM images of pristine n TiO$_2$.

Table 2 Retention rate in % of n TiO$_2$ inside the dialysis bags after 2 and 7 days of incubation in river water

	Retention rate in %		
Days	20 kDa ($\sim$5 nm)[a]	100 kDa ($\sim$10 nm)[a]	300 kDa ($\sim$20 nm)[a]
2	92.9 ($\pm$ 3.6)[b]	93.8 ($\pm$ 4.2)[b]	92.4 ($\pm$ 5.3)[b]
7	92.8 ($\pm$ 5.4)[b]	92.8 ($\pm$ 3.1)[b]	90.6 ($\pm$ 8.3)[b]

[a] There is no direct correlation between the pore dimension (nm) and the molecular size cut off (kDa); however, the manufacturer provides some approximations.[28] [b] Standard deviation.

The permeability of the membrane to dissolved organic matter (DOM) *via* free diffusion was evaluated using three-dimensional excitation-emission-matrix fluorescence spectroscopy (EEM). Four typical excitation/emission peaks have been observed in surface waters:[43] α (Ex/Em $\sim$ 340/420), α' (Ex/Em $\sim$ 250/430), β (as a shoulder on the α peak Ex/Em $\sim$ 300/420), and ϒ (Ex/Em $\sim$ 280/350). Among them, α, and α' have been attributed to the carboxylic and phenolic groups, respectively,[16] β to weakly humified structures, simple phenols, coumarins and alkaloids,[44] and ϒ to proteins.[45] Fig. 2 depicts the EEM fluorescence map of the river water inside and outside of the dialysis bag (100 kDa) exposed to river water for 1 week. The similarity of the signals suggests that the DOM fluorophores are similar in terms of quantity and quality; therefore, the membrane is probably permeable to most components of DOM, including proteins (similar ϒ signals). These results suggest that a cut-off of 100 kDa is large enough for DOM in natural water to permeate. Since we kept the possibility to apply the present method to particles smaller than 20 nm but larger than 10 nm such as some n-TiO$_2$ found in sunscreens[5] and avoid the presence of small natural colloids with the DOM-coated n-TiO$_2$, 100 kDa was selected for further optimization.

The exposure time of the dialysis bags to the river water is another important factor to optimize. On the one hand, this time should be long enough to reach the equilibrium of DOM between inside and outside of the dialysis bags and to allow a sufficient reaction time for nanoparticles; on the other hand, it should be short enough not to cause the decomposition of the membrane (chemical- and bio-degradation) in the river water. The optimal exposure time depends on the molecular cut-off and on the environmental conditions. Fig. 3 (left axis) shows the dissolved organic carbon (DOC) of the river sample (DOC around 6.5 ppm) inside and outside of dialysis bags initially filled with distilled water over one week under laboratory conditions. The initial DOC inside the dialysis bag was zero. Over time, the DOC inside the dialysis bag increased due to free diffusion of DOM from the river water toward inside the dialysis bag. By three hours, the measured DOC inside and outside of the dialysis bag became similar and remained stable, indicating that the system reached equilibrium in less than 3 h and up to 48 h. The difference between the DOC in the blank river water and with dialysis (about 13%) is probably due to organic leaching of the membrane and the closures.[46] This problem is not of relevance under field conditions since the volume of the water outside the bag is nearly infinite compared to the volume inside the membrane. Thus, the organic leaching cannot accumulate significantly near the bag.

After 48 h, there is a large increase in DOC concentration inside and outside the dialysis bag. This increase is most probably due to microbial activity leading to membrane decomposition[47] as suggested by the parallel decrease in dissolved oxygen (Fig. 3, right axis).[48] Since the parallel increase in DOC and decrease in dissolved oxygen were not
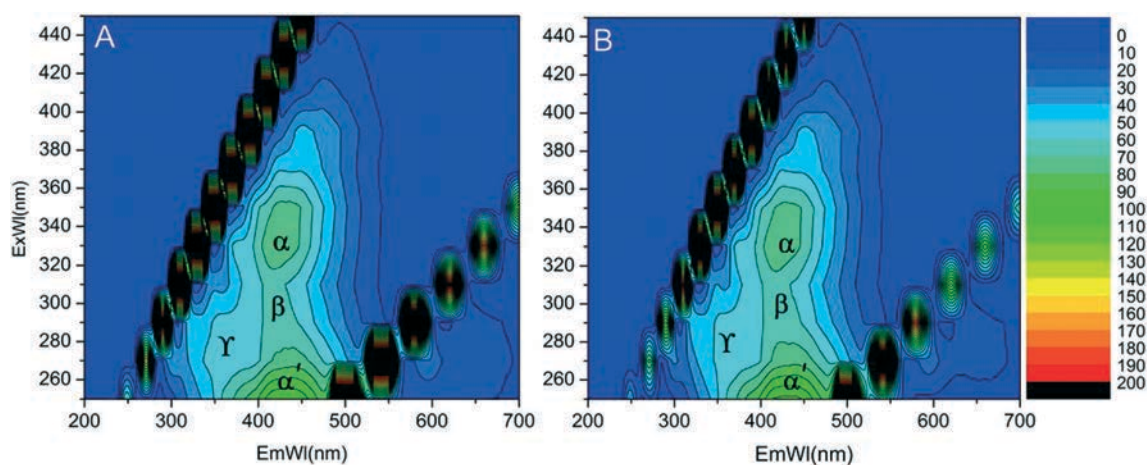
Fig. 2 Fluorescence EEMs A) inside and B) outside of the dialysis bag after one week of exposure to river water in the lab (the color scale depicts the intensity).
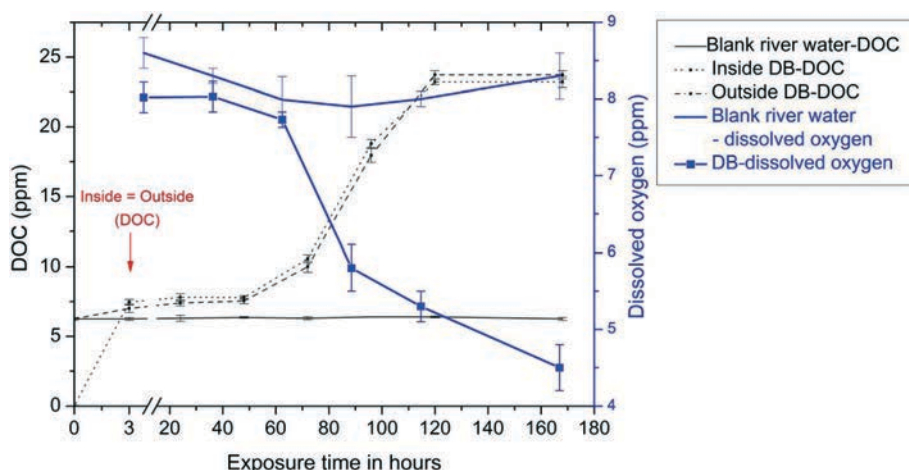
Fig. 3 DOC (left axis) and dissolved oxygen (right axis) of the river water inside and outside the dialysis bags (DB) initially filled with distilled water and immersed in river water at room temperature (error bars depict standard deviation).

observed in the blank river water, the dialysis bag is most probably the actual substrate for microbial development under conditions causing the membrane to decompose over time. In order to overcome this drawback for studies requiring exposure times longer than 48 h, we suggest modifying dialysis membranes to suppress microbial proliferation by using antibacterial agents in the membrane[47] or applying more robust membranes to microbial activity such as PVDF.

It has to be noted that, under different conditions (*e.g.* higher temperatures, high concentrations of nutrient, *etc.*), the decomposition of the membrane can be significantly faster. Therefore, we recommend keeping the exposure time as low as necessary for the equilibration of the DOC concentration inside the bag, while covering the relevant variations of environmental factors (*e.g.* day and night conditions) to be studied.

In addition to DOC and nanoparticles, the ability of inorganic ions to diffuse through the membrane was tested with river water under laboratory conditions after one week of exposure to river water. At room temperature, the pH remains stable inside and outside of the dialysis bag (pH = 7.2). However, the conductivity decreased by about 55% inside the bag. This can be due to the discrimination of some ions during the permeation or to bacterial growth.[49] To identify the source of this discrepancy, we determined the total concentration of a selection of the most common elements in surface waters inside and outside the dialysis bag using ICP-OES. For most monitored elements, the equilibrium could be reached, resulting in similar concentrations inside and outside the dialysis bags (Fig. 4). Notable exceptions are Al, Fe, and Mn whose total concentrations inside the bag decreased more compared to other elements (30–60%). This is probably due to their high valencies when present as ions (Al: +3, Fe: +2 and +3, Mn: +2, +4, and +7), which increases the probability to interact with the cellulose ester membrane.[50] On the other hand, these elements have been often observed as particulate matter,

colloidal or not, in surface waters,[51,52] which would drastically reduce their ability to diffuse through the membrane.

A complete equilibrium was reached for anion concentrations, as observed for the elements, except for nitrate with 20% reduction (Fig. 4). The highest reduction observed for nitrate can be due to the nitrate reduction caused by the microbial activity on the substrate of the dialysis bag after one week of exposure to river water.[53] Therefore, the observed decrease in conductivity can be partly due to a lower amount of natural colloids carrying charges and to lower nitrate concentration related to microbial activity, whereas other factors involving microbial activity cannot be ruled out.

Membrane fouling

Membrane fouling occurs when biotic or abiotic materials obstruct pores, thus reducing the permeability of the
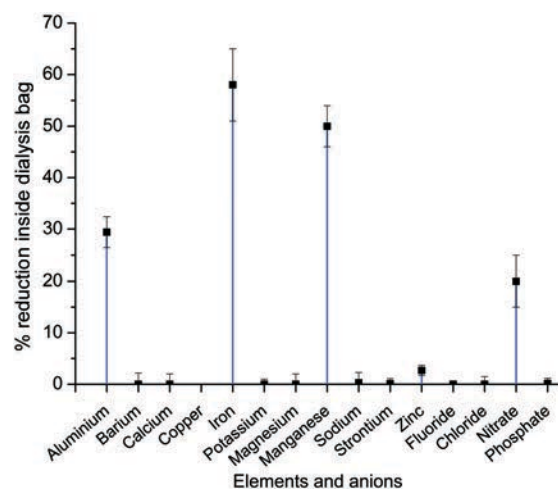

Fig. 4 The percentage of reduction of elements and anions by passing through the dialysis bags (compared to outside). Error bars depict standard deviation.

membrane. Fouling in natural waters, with a complex mixture of particulate and dissolved components, is one of the important processes reducing the permeability of membranes by reducing the pore size of the membrane.[54] Since drying of the membrane reduces drastically the pore size of dialysis membranes,[55] we determined the pore size of the membranes used for DOM exposure using NMR relaxometry and AFM under wet conditions.[56,57] NMR relaxometry enables an *in situ* estimation of a pore size distribution averaged over the whole sample, while AFM enables imaging of the pore system at some selected spots at the surface of the membrane. Therefore, the combination of these two complementary methods is highly valuable for obtaining information of the pore size under wet conditions.

Pore size distribution measured by NMR relaxometry

To investigate the probable effect of water medium (*e.g.* cations) on spin–spin relaxation time (T_2), bulk water media (distilled water and river water with and without n-TiO$_2$) were firstly measured (Fig. 5 – dash lines). There was no significant difference (*t*-test, 95%) in terms of T_2 distribution modes among the bulk media; therefore, the T_2 of water-filled pores was independent of the medium itself.

Fig. 5 (solid lines) depicts the T_2 measurements of water-filled pores of the dialysis bags in three different water media (distilled water and river water with and without n-TiO$_2$). In contrast to bulk water samples, the T_2 distributions of dialysis membrane samples depict two distinguished T_2 peaks representing the hierarchical structure in applied dialysis bags (cellulose ester).[30,58] Since the characteristic pore size of the membrane (r) and the T_2 of water-filled pores are proportional,[30] the larger T_2 (around 2000–3000 ms) indicates a slower relaxation and larger pores, and the smaller T_2 (200–300 ms) indicates a faster relaxation and
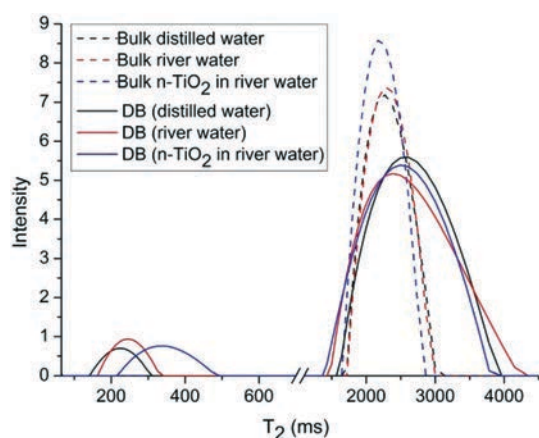
smaller pores. In addition, the larger T_2 distribution is the result of a mixed contribution between the water molecules absorbed on the surface of the membrane and free state; both states merge into one peak in the NMR relaxation spectra.[30]

Based on the *t*-test, we did not observe any significant difference in the T_2 distributions of dialysis membranes in different water media (distilled water and river water with and without n-TiO$_2$). This suggests that, under the applied conditions, the overall pore size of the dialysis bags does not change significantly. Therefore, the membrane fouling that causes the change in the pore size is negligible.

In order to verify that pore clogging can actually be detected using NMR relaxometry, measurements were performed with the membrane dried under ambient conditions. Since drying of the dialysis membrane is known to induce an irreversible collapse of the pores,[28] we expected the pore size to be drastically reduced after drying. Since the presence of water molecules in the pores is required for characterizing the pore size using NMR relaxometry, the dried membrane was rewetted for 24 hours prior to T_2 measurement. The first peak of the T_2 distribution corresponding to small pores of dried dialysis membranes after rewetting (Fig. 6-clogged pores) was significantly smaller (*t*-test, 95%) compared to that of non-dried membranes (Fig. 6-open pores). Considering a T_2 value for small pores around 70 ms as an extreme case for the collapse of the membrane structure, it can be concluded that all dialysis membrane samples in water media (Fig. 4-solid line) with T_2 values of 200–300 ms did not experience extended fouling, which would have led to a significant reduction of pore size.

Pore size distribution measured by AFM

Fig. 7 shows the AFM height and phase images of a dialysis membrane measured in distilled water. All the measurements were carried out in the fluid mode to avoid drying of the sample. Furthermore, this mode enables using the same media as those during the permeability experiments (river
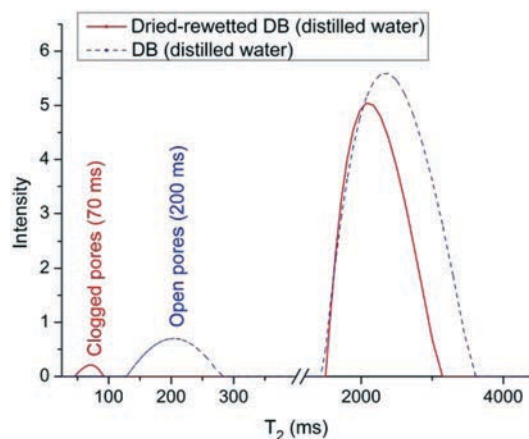
Fig. 5 NMR relaxation spectra (T_2) of the ^{1}H spins of the bulk samples of distilled water, river water, and n TiO$_2$ in river (dash line), and the water filled pores of dialysis bags (DB) incubated in the corresponding water media for one week (solid line). Each sample was measured in triplicate and the T_2 distributions are averaged over the corresponding replicates.

Fig. 6 T_2 distribution comparison of dried rewetted dialysis bags (clogged pores) and wet dialysis bags (open pores) in distilled water.
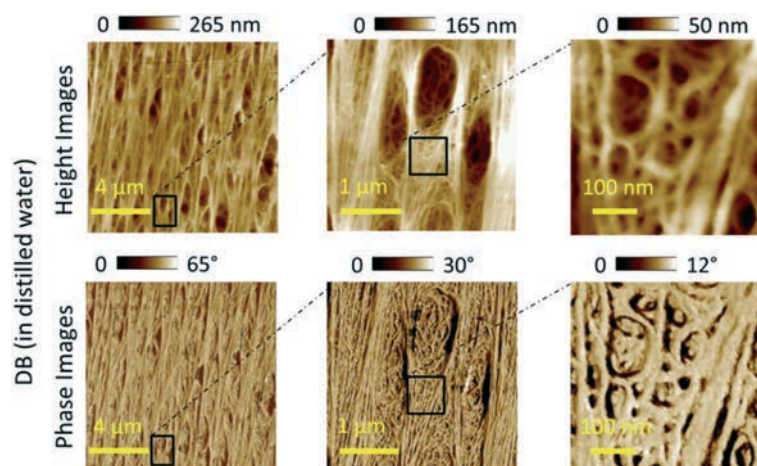
Fig. 7 AFM height (top) and phase (bottom) images of the dialysis bag (DB) in distilled water measured in fluid mode.

water with and without n-TiO$_2$), thus providing a more realistic assessment of the membrane pore size.

The images show the hierarchical porous structure of the dialysis bag. Three different areas are distinguishable in the images ranging from the nanometer to the micrometer scale: 1) a microporous structure with a polydisperse size distribution, 2) at higher magnification, a nanoporous network covering the whole sample including inside the micropores, and 3) a lamellar substructure. AFM images of dialysis bags in the river water (with and without n-TiO$_2$) depict an overall lower resolution compared to the samples measured in distilled water (Fig. S4 and S5†) probably due to ionic screening charges in river water (Bruker.com).

The pore size distribution of dialysis bags in different media (Fig. 8) shows a hydrodynamic diameter mode of 4 nm for all the samples. Besides, the observed differences between the pore sizes of the dialysis bags in different water media were not significant, in agreement with the results of NMR
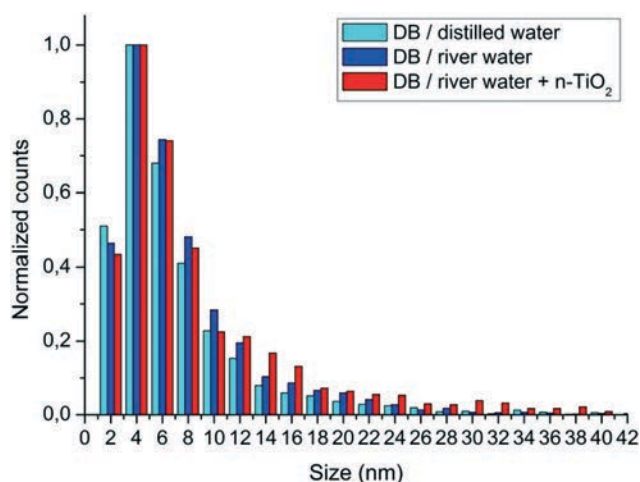
relaxometry. The determination of the average pore diameter of a three-dimensional porous structure based on two-dimensional images can only be an approximation based on several assumptions. Therefore, the absolute values of the pore size reported here should be taken as a first estimation and used for comparison purposes only.

Field experiment

Based on the previous method development, cylindrical cellulose ester dialysis bags with a MWCO of 100 kDa were chosen to carry out a proof of concept of investigating the interaction of n-TiO$_2$ with natural DOM under natural conditions. After one week of exposure in the river, the samples (inside the dialysis bag) were collected in polypropylene centrifuge tubes and transported immediately to the nearby laboratory. The n-TiO$_2$ nanoparticles were then separated using centrifugation for characterizing the sorption of NOM onto n-TiO$_2$. In general, the composition and quantity of DOM in natural waters vary over time[59] and investigations on the sorption require monitoring of these variations over the deployment period. However, the concentrations inside and outside the dialysis bag equilibrate in less than a few hours and the water composition was fairly stable over the time of this study (Table S1†). Hence, we assume that the compositions of water sampled outside and inside the dialysis bag are similar. To provide a reference for NOM (outside the dialysis bag), the river water was also collected in polypropylene centrifuge tubes on the last day of exposure.

Permeability of the membrane under the field experiment: fluorescence EEMs

Fig. 9 shows the fluorescence EEMs of the river water (A) and the river water diffused into the dialysis bag (B). In both samples, the EEM plots show four spectral features of the natural waters related to α, α′, β, and ϒ corresponding

Fig. 8 Pore size distribution of dialysis bags (DB) in different water media determined using AFM in fluid mode (six AFM regions of interest were used for each sample).
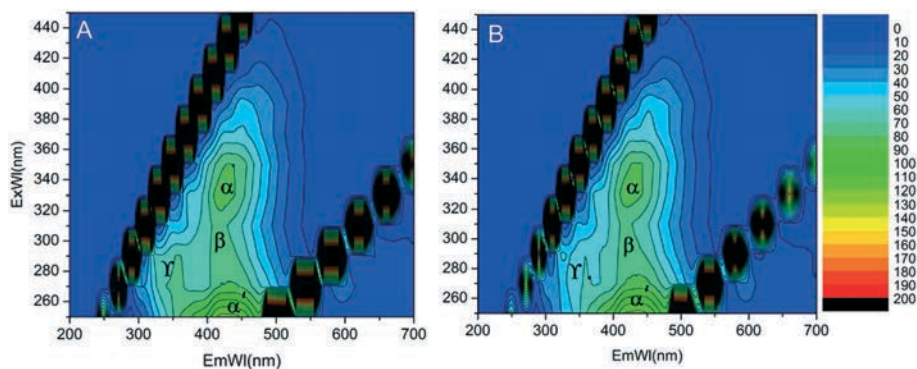
Fig. 9 Fluorescence EEMs of the samples carried out in the field: A) river water and B) river water inside the dialysis bag (the color scale depicts the intensity in a.u).

respectively to carboxylic, phenolic, alkaloids, and protein groups (see the discussion above).

As can be seen, the α, α′, and β peaks of the river water are similar inside and outside of the DB. It can suggest that the composition of DOM of the river water inside the DB is similar to that of the natural water to a good extent.

Fig. S6† depicts the fluorescence EEM of the supernatant of the river water inside DB in the presence of n-TiO₂. All the mentioned peaks in the river water (α, α′, β, and ϒ) are present with reduced intensities in this sample. An indirect effect of the sorption of DOM onto n-TiO₂ could explain these differences. However, one should notice that the quantitative interpretation of fluorescence results for such complex mixtures is far from trivial and should be considered as a first approach in the frame of this proof of concept. Hence, the fluorescence EEM results can be investigated qualitatively not quantitatively. However, the results show that the DOM permeates the membrane under field conditions and the observations made are similar to the ones made in the lab. The biological activities induced by the membrane decomposition seem not to impair sensibly the permeability of the membrane and may, therefore, be of little importance under field conditions.
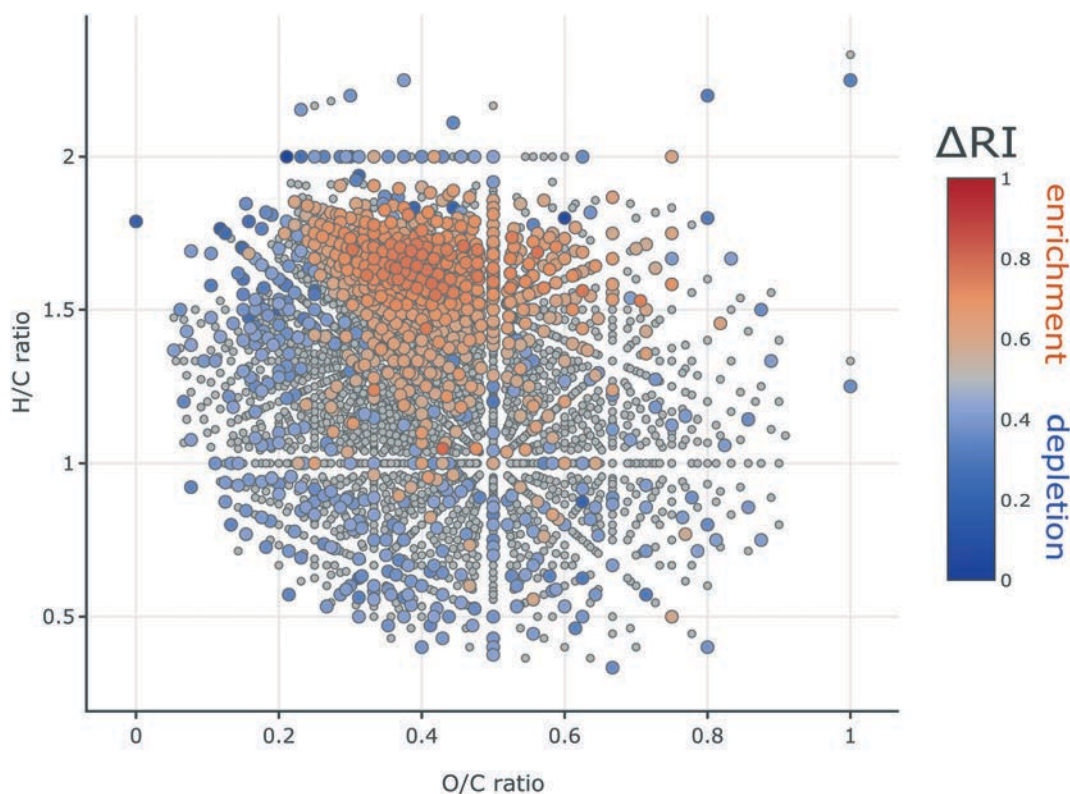

Fig. 10 Van Krevelen diagram with intensity differences for river water inside the dialysis bags *vs.* river water. ΔRI values above 0.57 (red) were considered to indicate that the respective compound is enriched inside the dialysis bags, and ΔRI values below 0.43 (blue) indicate that the respective compound is depleted inside the dialysis bag.

Since the results of fluorescence spectroscopy just express the fluorophore groups in the river water, and the activity of lipids or polysaccharides, for instance, cannot be monitored, the water media were further investigated with FT-ICR-MS.

Permeability of the membrane under the field experiment: FT-ICR-MS

Ultrahigh resolution Fourier-transform ion cyclotron resonance mass spectrometry (FT-ICR-MS) was used to gain detailed insight into the molecular composition of river water DOM inside and outside the dialysis bag.

3766 (58%) out of 6468 formulas were shared between all three river samples (outside the dialysis bag, and inside the dialysis bag with and without n-TiO$_2$), while 1181 (18%) and 1539 (24%) formulas occurred only in one and two samples, respectively (Fig. S7†). As expected for terrestrial derived DOM, there was a large dominance of CHO (53%) compounds over CHNO (35%) and CHOS (10%) (Table S4†).

Some compounds were depleted (ΔRI < 0.43) in the water outside *vs.* inside the bag (n = 554) but showed a homogenous distribution in the van Krevelen (vK) space as expected for analytical noise (Fig. 10). However, based on intensity differences between river water inside the dialysis bags and river water outside the bags, there emerges a clear pattern for compounds enriched inside the bags (ΔRI > 0.57, n = 591). They represent compounds which are highly aliphatic (H/C = 1.622 ± 0.178), and cover a broad range of oxygenation (O/C = 0.403 ± 0.108).

Cellulose acetate is biodegradable in the presence of esterases which is produced by different classes of microorganisms.[60] Upon biodegradation, cellulose acetate undergoes deacetylation and break down of the cellulose backbone[61] into smaller chains or glucose monomers, which are potential sources of energy for further microbial activities. Hence, the observed pattern of enriched compounds inside the dialysis bag (compared to the river water) may point to microbial induced degradation of the membrane. This is in agreement with the results of DOC and dissolved O$_2$ (Fig. 3) showing respiration within and DOC leaching from the bag in one week under laboratory conditions.

Interestingly, compounds with similar chemical properties (H/C = 1.539 ± 0.368, O/C = 0.401 ± 0.148) were depleted when n-TiO$_2$ was added to the bags compared to the bags without n-TiO$_2$ (Fig. S8†) *i.e.* the enrichment observed in the river water inside the dialysis bag is not observed with n-TiO$_2$ present. While the enriched compounds inside the bag are mostly CHO (73%), the depleted compounds with n-TiO$_2$ contain a larger fraction of CHNO formulas (47%). In the field experiment, under the assumption of thermodynamic equilibrium, any preferential sorption of DOM on the n-TiO$_2$ can be compensated for by river water from outside the dialysis bag. This assumption is acceptable considering the relatively short equilibration time measured in the laboratory experiments (less than 3 h, Fig. 3) and the stability of the

river water chemical parameters over months (Table S1†). Therefore, the observed differences in DOM composition are probably not related only to sorption, but also to the effect of n-TiO$_2$ on the biodegradation of the membrane. Indeed, Lazic *et al.* reported the negative influence of n-TiO$_2$ on biodegradation of cellulose.[62]

In order to explore this hypothesis, we determined the measured DOC and dissolved oxygen (DO) of the river water inside the dialysis bag with and without n-TiO$_2$ over a week under laboratory conditions (Fig. S9†). In both cases, DOC was increasing over a week; however, less increase was observed in the presence of n-TiO$_2$. Since the control samples of the river water with and without n-TiO$_2$ showed a similar DOC, sorption cannot be the determinant factor of the decreased DOC production inside the bag in the presence of nanoparticles. Furthermore, a DOC increase occurred parallel to a DO decrease (Fig. S9†) with less reduction observed inside the dialysis bag in the presence of n-TiO$_2$ while the control samples of the river water with and without n-TiO$_2$ showed almost the same DO. Therefore, we conclude that n-TiO$_2$ reduces the biodegradation of cellulose ester under laboratory and field conditions.

Sorption of DOM onto n-TiO$_2$: ATR-FTIR

The ATR-FTIR spectra of n-TiO$_2$ and n-TiO$_2$ exposed to the river water are shown in Fig. 11. There are two bands in both samples, the peak around 1640 cm^{-1} is attributed to the bending vibration of the O–H bond of chemisorbed water and the broad peak around 3350 cm^{-1} corresponds to the surface adsorbed water and hydroxyl groups. A prominent band occurring at 430 cm^{-1} due to Ti–O and Ti–O–Ti stretching vibration modes is shifted to lower frequency after exposure to river water,[63] probably due to the interaction of Ti–O with the DOM of the river water. The major functional
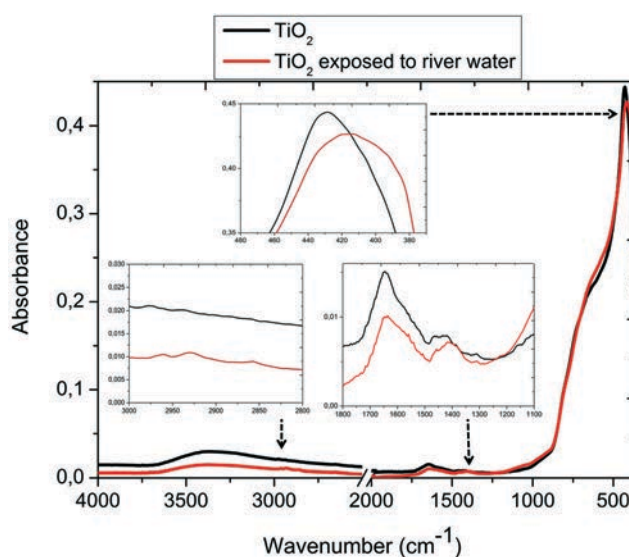

Fig. 11 ATR FTIR spectra of n TiO$_2$ and n TiO$_2$ exposed to river water in the field experiment.

Table 3 Elemental content (CHNS) in river water, n TiO$_2$, and n TiO$_2$ exposed to river water

Element content (wt%)	n TiO$_2$	n TiO$_2$ exposed to river water	River water
C	0.012	1.23	6.15
H	0.057	0.18	1.53
N	0.107	0.26	1.29
S	0.13	0.74	4.84

groups in aquatic humic substances are carboxylic acid, hydroxyl, phenolic, and carbonyl groups (1100–1700 cm ^{1}),[26] which were seen in the river water sample (Fig. S10†). After exposing n-TiO$_2$ to the river water, we observed a shift in the band at 1400–1450 cm ^{1} (Fig. 11) which could be attributed to carboxylic acid groups, which were also present in the river water (Fig. S10†). The C–H stretching vibrations (CH$_2$) between 2950 and 2850 clearly indicate the presence of absorbed organic matter. However, these bands were not prominent in the river water spectrum (Fig. S10†); therefore it is not clear if the observed CH$_2$ groups correspond to absorbed organic matter from the river water. In addition, the agglomeration of the nanoparticles in the river media could cause the observed band broadening.[64] Therefore, CHNS analyses were carried out in order to confirm that natural organic matter from the river water sorbed onto the n-TiO$_2$.

Sorption of DOM onto n-TiO$_2$: CHNS

Elemental analysis in Table 3 depicts the carbon, nitrogen, hydrogen, and sulfur contents of river water (freeze-dried), n-TiO$_2$, and n-TiO$_2$ exposed to river water. The CHNS-contents in n-TiO$_2$ exposed to river water were higher than those in pristine n-TiO$_2$ probably indicating the sorption of DOM onto n-TiO$_2$. Fig. 12 shows that the Euclidean distances allow the comparison of the elemental composition of the three treatments, where "A" is assigned to n-TiO$_2$, "B" to river water, and "C" to n-TiO$_2$ exposed to river water (A–B: 0.495 ± 0.25, A–C: 0.528 ± 0.24, B–C: 0.0965 ± 0.18). Since the point corresponding to n-TiO$_2$ exposed to river water is closer to the river water than to the pristine n-TiO$_2$ (Fig. 12: B–C < A–C), we conclude that the organic matter adsorbed onto the
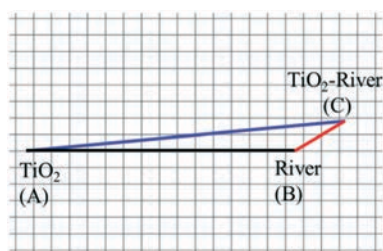

Fig. 12 Euclidean distances calculated from the normalized C , H , N , and S contents (four dimensional space) of river water, n TiO$_2$, and n TiO$_2$ exposed to river water where A B: 0.495 ± 0.25, A C: 0.528 ± 0.24, B C: 0.0965 ± 0.18.

nanoparticles under field conditions does not experience strong fractionation. This results in an NOM-coating chemically close to river water DOM. Furthermore, comparing the absolute absorbance values of the elements showed that although there is a high difference between the amount of river water in two samples of "B" and "C" (250 ml of freeze-died river water in "B" compared to a few μL of residual river water on n-TiO$_2$ in "C"), the absorbance is comparable. Hence, the contribution of the residual river water to the CHNS-signal of the nanoparticles in river water is negligible. Combining the hints provided by EEM fluorescence, ATR-FTIR, and CHNS analyses, we can conclude that the sorption of DOM occurred under field conditions and that the proposed concept is valid.

Conclusion

In this work, we introduced a dialysis membrane as a passive reactor to produce nanoparticles with natural coating. Such particles could be useful to study the fate and toxicity of nanoparticles under natural conditions. Since nanoparticles from 20 nm are successfully retained in the reactor and most of the DOM can permeate through the membrane and reach the nanoparticle surface, we conclude that the concept is valid. Furthermore, the sorption of DOM onto n-TiO$_2$ was evaluated by ATR-FTIR and CHNS elemental analysis of the nanoparticles before and after exposure to the river water which both depicted the occurrence of sorption under applied conditions. Further validation will include testing the performance of the reactor under various conditions and in differing surface waters. For exposure times longer than two days, the microbial activity due to the degradation of the membrane may interfere with the sorption processes. Optimizing the membrane properties and sample preparation in order to minimize this effect can help in this respect. Finally, for future studies, more advanced analytical methods are required to characterize NOM-engineered nanoparticle corona.

Conflicts of interest

There are no conflicts to declare.

Acknowledgements

References

1 N. C. Birben, C. S. Uyguner-Demirel, S. S. Kavurmaci, Y. Y. Gürkan, N. Turkten, Z. Cinar and M. Bekbolet, Application Fe-doped TiO_2 specimens for the solar photocatalytic degradation of humic acid, *Catal. Today*, 2017, **281**, 78–84.

2 F. Loosli, P. Le Coustumer and S. Stoll, Effect of electrolyte valency, alginate concentration and pH on engineered TiO_2 nanoparticle stability in aqueous solution, *Sci. Total Environ.*, 2015, **535**, 28–34.

3 V. Adam, S. Loyaux-Lawniczak and G. Quaranta, Characterization of engineered TiO_2 nanomaterials in a life cycle and risk assessments perspective, *Environ. Sci. Pollut. Res.*, 2015, **22**, 11175–11192.

4 Y. S. Sahu, *Nano Titanium Dioxide Market by Application (Paints & Coatings, Pigments, Cosmetics, Plastics, Energy and others) - Global Opportunity Analysis and Industry Forecast, 2014–2022*, Allied Market Research, 2016, p. 119.

5 A. Philippe, J. Košík, A. Welle, J.-M. Guigner, O. Clemens and G. E. Schaumann, Extraction and characterization methods for titanium dioxide nanoparticles from commercialized sunscreens, *Environ. Sci.: Nano*, 2018, **5**, 191–202.

6 A. P. Gondikas, F. von der Kammer, R. B. Reed, S. Wagner, J. F. Ranville and T. Hofmann, Release of TiO_2 nanoparticles from sunscreens into surface waters: a one-year survey at the old Danube recreational Lake, *Environ. Sci. Technol.*, 2014, **48**, 5415–5422.

7 M. Bundschuh, J. Filser, S. Lüderwald, M. S. McKee, G. Metreveli, G. E. Schaumann, R. Schulz and S. Wagner, Nanoparticles in the environment: where do we come from, where do we go to?, *Environ. Sci. Eur.*, 2018, **30**, 6.

8 G. E. Schaumann, A. Philippe, M. Bundschuh, G. Metreveli, S. Klitzke, D. Rakcheev, A. Grün, S. K. Kumahor, M. Kühn and T. Baumann, others, Understanding the fate and biological effects of Ag-and TiO_2-nanoparticles in the environment: the quest for advanced analytics and interdisciplinary concepts, *Sci. Total Environ.*, 2015, **535**, 3–19.

9 A. Philippe and G. E. Schaumann, Interactions of dissolved organic matter with natural and engineered inorganic colloids: a review, *Environ. Sci. Technol.*, 2014, **48**, 8946–8962.

10 C. Zhang, J. Lohwacharin and S. Takizawa, Properties of residual titanium dioxide nanoparticles after extended periods of mixing and settling in synthetic and natural waters, *Sci. Rep.*, 2017, **7**, 9943.

11 S. Valencia, J. M. Marín, G. Restrepo and F. H. Frimmel, Evaluation of natural organic matter changes from Lake Hohloh by three-dimensional excitation-emission matrix fluorescence spectroscopy during TiO_2/UV process, *Water Res.*, 2014, **51**, 124–133.

12 N. Sani-Kast, J. Labille, P. Ollivier, D. Slomberg, K. Hungerbühler and M. Scheringer, A network perspective reveals decreasing material diversity in studies on nanoparticle interactions with dissolved organic matter, *Proc. Natl. Acad. Sci. U. S. A.*, 2017, 201608106.

13 C. Nickel, B. Hellack, A. Nogowski, F. Babick, M. Stintz, H. Maes, A. Schäffer and T. Kuhlbusch, *Mobility, fate and behavior of TiO_2 nanomaterials in different environmental media*, Environmental Research of the Federal Ministry for the Environment, 2013.

14 M. Luo, Y. Huang, M. Zhu, Y. Tang, T. Ren, J. Ren, H. Wang and F. Li, Properties of different natural organic matter influence the adsorption and aggregation behavior of TiO_2 nanoparticles, *J. Saudi Chem. Soc.*, 2018, **22**, 146–154.

15 M. Drosos, M. Ren and F. H. Frimmel, The effect of NOM to TiO_2: interactions and photocatalytic behavior, *Appl. Catal., B*, 2015, **165**, 328–334.

16 W. Chen, C. Qian, X.-Y. Liu and H.-Q. Yu, Two-dimensional correlation spectroscopic analysis on the interaction between humic acids and TiO_2 nanoparticles, *Environ. Sci. Technol.*, 2014, **48**, 11119–11126.

17 S. Shakiba, A. Hakimian, L. R. Barco and S. M. Louie, Dynamic Intermolecular Interactions Control Adsorption from Mixtures of Natural Organic Matter and Protein onto Titanium Dioxide Nanoparticles, *Environ. Sci. Technol.*, 2018, **52**, 14158–14168.

18 J. Namieśnik, B. Zabiegała, A. Kot-Wasik, M. Partyka and A. Wasik, Passive sampling and/or extraction techniques in environmental analysis: a review, *Anal. Bioanal. Chem.*, 2005, **381**, 279–301.

19 A. Kot, B. Zabiegala and J. Namiesnik, Passive sampling for long-term monitoring of organic pollutants in water, *TrAC, Trends Anal. Chem.*, 2000, **19**, 446–459.

20 T. Górecki and J. Namie'snik, Passive sampling, *TrAC, Trends Anal. Chem.*, 2002, **21**, 276–291.

21 D. A. Vroblesky, J. Manish, J. Morrell and J. Peterson, Evaluation of passive diffusion bag samplers, dialysis samplers, and nylon-screen samplers in selected wells at Andersen Air Force Base, Guam, March-April 2002, *US Geological Survey Water-Resources Investigations Report*, 2003, pp. 03–4157.

22 B. E. Vencalek, S. N. Laughton, E. Spielman-Sun, S. M. Rodrigues, J. M. Unrine, G. V. Lowry and K. B. Gregory, In situ measurement of CuO and $Cu(OH)_2$ nanoparticle dissolution rates in quiescent freshwater mesocosms, *Environ. Sci. Technol. Lett.*, 2016, **3**, 375–380.

23 P. Benes and E. Steinnes, In situ dialysis for the determination of the state of trace elements in natural waters, *Water Res.*, 1974, **8**, 947–953.

24 P. Wang, Aggregation of TiO_2 Nanoparticles in Aqueous Media: Effects of pH, Ferric Ion and Humic Acid, *Int. J. Environ. Sci. Nat. Res.*, 2017, **1**, 555575.

25 W. Wu, G. Shan, Q. Xiang, Y. Zhang, S. Yi and L. Zhu, Effects of humic acids with different polarities on the photocatalytic activity of nano-TiO_2 at environment relevant concentration, *Water Res.*, 2017, **122**, 78–85.

26 K. J. Howe, K. P. Ishida and M. M. Clark, Use of ATR/FTIR spectrometry to study fouling of microfiltration membranes by natural waters, *Desalination*, 2002, **147**, 251–255.

27 S. Jeon, S. Rajabzadeh, R. Okamura, T. Ishigami, S. Hasegawa, N. Kato and H. Matsuyama, The effect of membrane material and surface pore size on the fouling properties of submerged membranes, *Water*, 2016, **8**, 602.

28 https://www.repligen.com/dialysis-tubing-membranes.

29 M. Meyer, C. Buchmann and G. Schaumann, Determination of quantitative pore-size distribution of soils with 1H NMR relaxometry, *Eur. J. Soil Sci.*, 2018, **69**, 393–406.

30 C. Zhang, P. Li, Y. Zhang, F. Lu, W. Li, H. Kang, J. Xiang, Y. Huang and R. Liu, Hierarchical porous structures in cellulose: NMR relaxometry approach, *Polymer*, 2016, **98**, 237–243.

31 J. V. Bayer, F. Jaeger and G. E. Schaumann, Proton nuclear magnetic resonance (NMR) relaxometry in soil science applications, *Open Magn. Reson. J.*, 2010, **3**, 15–26.

32 http://www.nanophys.kth.se/nanophys/facilities/nfl/afm/fast-scan/bruker-help/Content/Probe%20and%20Sample%20Guide/Samples/FS%20Fluid%20Sample%20Mounting.htm.

33 http://www.nanophys.kth.se/nanophys/facilities/nfl/afm/fast-scan/brukerhelp/Content/Fluid%20Imaging/FS%20Fluid%20Operation Droplet.htm.

34 R. J. Peters, G. van Bemmel, N. B. Milani, G. C. den Hertog, A. K. Undas, M. van der Lee and H. Bouwmeester, Detection of nanoparticles in Dutch surface waters, *Sci. Total Environ.*, 2018, **621**, 210–218.

35 J. Raeke, O. J. Lechtenfeld, M. Wagner, P. Herzsprung and T. Reemtsma, Selectivity of solid phase extraction of freshwater dissolved organic matter and its effect on ultrahigh resolution mass spectra, *Environ. Sci.: Processes Impacts*, 2016, **18**, 918–927.

36 O. J. Lechtenfeld, G. Kattner, R. Flerus, S. L. McCallister, P. Schmitt-Kopplin and B. P. Koch, Molecular transformation and degradation of refractory dissolved organic matter in the Atlantic and Southern Ocean, *Geochim. Cosmochim. Acta*, 2014, **126**, 321–337.

37 B. Koch, G. Kattner, M. Witt and U. Passow, Molecular insights into the microbial formation of marine dissolved organic matter: recalcitrant or labile?, *Biogeosciences*, 2014, **11**, 4173–4190.

38 P. Herzsprung, N. Hertkorn, W. von Tümpling, M. Harir, K. Friese and P. Schmitt-Kopplin, Understanding molecular formula assignment of Fourier transform ion cyclotron resonance mass spectrometry data of natural organic matter from a chemical point of view, *Anal. Bioanal. Chem.*, 2014, **406**, 7977–7987.

39 P. Herzsprung, N. Hertkorn, W. von Tümpling, M. Harir, K. Friese and P. Schmitt-Kopplin, Molecular formula assignment for dissolved organic matter (DOM) using high-field FT-ICR-MS: chemical perspective and validation of sulphur-rich organic components (CHOS) in pit lake samples, *Anal. Bioanal. Chem.*, 2016, **408**, 2461–2469.

40 T. Kind and O. Fiehn, Seven Golden Rules for heuristic filtering of molecular formulas obtained by accurate mass spectrometry, *BMC Bioinf.*, 2007, **8**, 105.

41 J. Raeke, O. J. Lechtenfeld, J. Tittel, M. R. Oosterwoud, K. Bornmann and T. Reemtsma, Linking the mobilization of dissolved organic matter in catchments and its removal in drinking water treatment to its molecular characteristics, *Water Res.*, 2017, **113**, 149–159.

42 M. Kosmulski, Isoelectric points and points of zero charge of metal (hydr) oxides: 50 years after Parks' review, *Adv. Colloid Interface Sci.*, 2016, **238**, 1–61.

43 B. Matthews, A. Jones, N. Theodorou and A. Tudhope, Excitation-emission-matrix fluorescence spectroscopy applied to humic acid bands in coral reefs, *Mar. Chem.*, 1996, **55**, 317–332.

44 P. Boguta and Z. Sokołowska, Interactions of Zn(II) ions with humic acids isolated from various type of soils. Effect of pH, Zn concentrations and humic acids chemical properties, *PLoS One*, 2016, **11**, e0153626.

45 M. Sierra, M. Giovanela, E. Parlanti and E. Soriano-Sierra, Fluorescence fingerprint of fulvic and humic acids from varied origins as viewed by single-scan and excitation/emission matrix techniques, *Chemosphere*, 2005, **58**, 715–733.

46 E. Khan and S. Subramania-Pillai, Effect of leaching from filters on laboratory analyses of collective organic constituents, *Proceedings of the Water Environment Federation*, 2006, vol. 2006, pp. 901–918.

47 A. F. de Faria, A. C. M. de Moraes, P. F. Andrade, D. S. da Silva, M. do Carmo Gonçalves and O. L. Alves, Cellulose acetate membrane embedded with graphene oxide-silver nanocomposites and its ability to suppress microbial proliferation, *Cellulose*, 2017, **24**, 781–796.

48 http://www.epa.gov/glindicators/water/oxygenb.html, *Dissolved Oxygen Depletion in Lake Erie, In Great Lakes Monitoring*.

49 K. Krishnamurti and S. Kate, Changes in electrical conductivity during bacterial growth, *Nature*, 1951, **168**, 170.

50 K. Andarany, A. Sagir, A. Ahmad, S. Deni and W. Gunawan, in *IOP Conference Series: Materials Science and Engineering*, 2017, vol. 237, p. 012042.

51 B. M. Tebo, J. R. Bargar, B. G. Clement, G. J. Dick, K. J. Murray, D. Parker, R. Verity and S. M. Webb, Biogenic manganese oxides: properties and mechanisms of formation, *Annu. Rev. Earth Planet. Sci.*, 2004, **32**, 287–328.

52 T. Rennert, Wet-chemical extractions to characterise pedogenic Al and Fe species-a critical review, *Soil Res.*, 2019, **57**, 1–16.

53 M. Tiso and A. N. Schechter, Nitrate reduction to nitrite, nitric oxide and ammonia by gut bacteria under physiological conditions, *PLoS One*, 2015, **10**, e0119712.

54 E. Fridjonsson, S. Vogt, J. S. Vrouwenvelder and M. Johns, Early non-destructive biofouling detection in spiral wound RO membranes using a mobile earth's field NMR, *J. Membr. Sci.*, 2015, **489**, 227–236.

55 Y. Qing, R. Sabo, Y. Wu, J. Zhu and Z. Cai, Self-assembled optically transparent cellulose nanofibril films: effect of nanofibril morphology and drying procedure, *Cellulose*, 2015, **22**, 1091–1102.

56 M. Hayama, K. Yamamoto, F. Kohori and K. Sakai, How polysulfone dialysis membranes containing polyvinylpyrrolidone achieve excellent biocompatibility?, *J. Membr. Sci.*, 2004, **234**, 41–49.

57 L. A. Neves, P. J. Sebastiao, I. M. Coelhoso and J. G. Crespo, Proton NMR relaxometry study of nafion membranes modified with ionic liquid cations, *J. Phys. Chem. B*, 2011, **115**, 8713–8723.

58 S. Polarz, B. Smarsly and J. H. Schattka, Hierachical porous carbon structures from cellulose acetate fibers, *Chem. Mater.*, 2002, **14**, 2940–2945.

59 H. Van de Weerd, W. Van Riemsdijk and A. Leijnse, Modeling the dynamic adsorption/desorption of a NOM mixture: Effects of physical and chemical heterogeneity, *Environ. Sci. Technol.*, 1999, **33**, 1675–1681.

60 K. Sayali, P. Sadichha and S. Surekha, Microbial esterases: an overview, *Int. J. Curr. Microbiol. Appl. Sci.*, 2013, **2**, 135–146.

61 J. Puls, S. A. Wilson and D. Hölter, Degradation of Cellulose Acetate-Based Materials: A Review, *J. Polym. Environ.*, 2011, **19**, 152–165.

62 V. Lazic, M. Radoicic, Z. Saponjic, T. Radetic, V. Vodnik, S. Nikolic, S. Dimitrijevic and M. Radetic, Negative influence of Ag and TiO_2 nanoparticles on biodegradation of cotton fabrics, *Cellulose*, 2015, **22**, 1365–1378.

63 L. Saravanan, R. M. Kumar, A. Pandurangan and R. Jayavel, Synthesis and photophysical studies of PVP capped Titania Nanostrips for photocatalytic applications, *Optoelectron. Adv. Mater., Rapid Commun.*, 2010, **4**, 1676–1680.

64 K. S. Babu, A. R. Reddy, C. Sujatha, K. V. Reddy and A. Mallika, Synthesis and optical characterization of porous ZnO, *J. Adv. Ceram.*, 2013, **2**, 260–265.

Repository KITopen

Dies ist ein Postprint/begutachtetes Manuskript.

Empfohlene Zitierung:

Tayyebi Sabet Khomami, N.; Philippe, A.; Abu Quba, A. A.; Lechtenfeld, O. J.; Guigner, J.-M.; Heissler, S.; Schaumann, G. E.
Validation of a field deployable reactor for in situ formation of NOM-engineered nanoparticle corona.
2020. Environmental science / Nano, 7.
doi:10.5445/IR/1000105946

Zitierung der Originalveröffentlichung:

Tayyebi Sabet Khomami, N.; Philippe, A.; Abu Quba, A. A.; Lechtenfeld, O. J.; Guigner, J.-M.; Heissler, S.; Schaumann, G. E.
Validation of a field deployable reactor for in situ formation of NOM-engineered nanoparticle corona.
2020. Environmental science / Nano, 7 (2), 486–500.
doi:10.1039/c9en01090d